EPJ Web of Conferences **60**, 08001 (2013)
DOI: 10.1051/epjconf/20136008001

W and Z precision physics

M.Isabel Josa[1,a] for the ATLAS, CMS and LHCb collaborations

[1] *CIEMAT, Centro de Investigaciones Energéticas, Medioambientales y Tecnológicas. Avda. Complutense 40, 28040 - Madrid, Spain*

Abstract. Recent results on W and Z physics from LHC experiments are presented. Measurements reviewed include total W and Z cross sections, W lepton charge asymmetry, and Z differential cross sections. Production of Z bosons is studied as a function of rapidity, transverse momentum and angular variables. The Drell-Yan differential distribution with the dilepton mass and the double differential distribution with the dilepton mass and rapidity are shown. Finally, measurements of several electroweak observables, the forward-backward Drell-Yan asymmetry and the $\sin\theta_W$ are also presented. The measurements are compared with theoretical predictions using the most accurate theoretical predictions and modern parton distribution functions. A general agreement is observed.

1 Introduction

The high production rate of W and Z and their clean decay signatures, mainly in the leptonic channels make these processes an excellent tool for Physics commissioning at the LHC energy regime. Detector performance, in terms of lepton reconstruction (trigger, reconstruction and identification efficiencies) and calibration of lepton energy and momentum is now routinely studied with samples of Z candidates. The presence of a neutrino in the final state from the decay of a W boson, and hence of a natural source of missing transverse energy in the event is also employed for the characterization of this physical quantity. From the theory side they are well known processes and precise predictions are available, making them an excellent testbench of the Standard Model at the LHC energy. Furthermore, W and Z bosons are produced in numerous relevant processes being studied at LHC and constitute one of the most copious backgrounds for BSM searches, thus a detailed knowledge of their kinematic and dynamic characteristics is needed.

W and Z production proceeds at Leading-Order (LO) through the scattering of a u or d valence quark with a sea-antiquark. At the LHC energy, the accessible range of the momentum fraction of the proton carried by the interacting partons (x), increases significantly with respect to previous experiments, and the contribution from sea-quark sea-antiquark starts to be significant. In this sense, W and Z production gives access to probe and constrain Parton Distribution Functions (PDF) in enlarged regions. The three LHC experiments: ATLAS and CMS, and LHCb provide complementary information. Vector boson production in ATLAS and CMS covers an x range $\sim (0.5\times10^{-4} - 10^{-1})$ and the forward design of LHCb extends the coverage down to $x \sim 10^{-4}$.

The large statistical samples collected during the 2011 LHC run: 40M W $\rightarrow \ell\nu$, 3M Z $\rightarrow \ell\ell$ (0.6M, 50k in the very forward region) opened the possibility to perform rather detailed differential measurements. Systematic uncertainties are of the order of 1% for inclusive measurements and of few % for differential ones, excluding the uncertainty arising from the determination of the integrated luminosity, that ranges from $\sim$ 2.2% to 4% depending on the experiment and period. Better precision is achieved in ratios where some of the systematic uncertainties cancel out completely (the one due to the luminosity determination) and the effect from the other sources is reduced. Measurements are usually performed in a restricted phase space where detection is optimal. They are extrapolated to the full phase space by means of correction factors computed with the theoretical tools available, that are determined with $\sim 1-2\%$ uncertainty. Therefore experiments also quote their results in the restricted fiducial phase space to minimize uncertainties and to allow a precise comparison with theoretical predictions.

Several tools are available to produce theoretical predictions at Next-to-Next-to-Leading-Order (NNLO) (FEWZ [1] and DYNNLO [2]) with a precision already comparable to the experimental one (few percent). Signal modeling is significantly improved in Montecarlo generators such as POWHEG [3] or MC@NLO [4] that incorporate a NLO description of the process.

Selection of W and Z candidates is relatively simple. Both ATLAS and CMS base their selection on high p_T isolated leptons that in the case of the W candidates is accompanied by an apparent imbalance in the energy of the event. Typically $p_T(\mu) > 20$ (25) GeV for ATLAS (CMS) and $p_T(e) > 25$ GeV both for ATLAS and CMS.

[a] e-mail: Isabel.Josa@ciemat.es

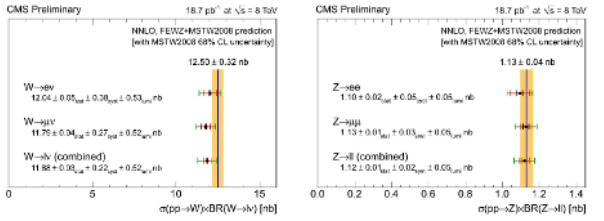

Figure 1. Summary of the W and Z production cross section times the leptonic branching fractions at $\sqrt{s} = 8\,\text{TeV}$. Measurements in the electron and muon channels, and combined, are compared to the theoretical predictions computed at the NNLO in QCD with FEWZ and MSTW2008 PDF set.

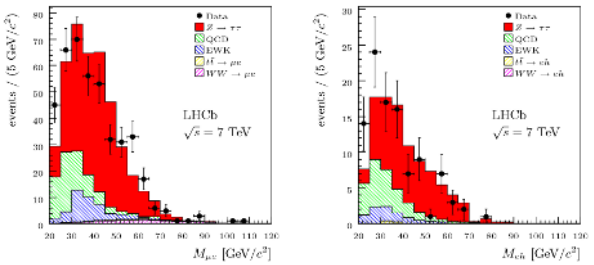

Figure 2. Invariant mass distributions $\tau_\mu\tau_e$ (left) and $\tau_\mu\tau_h$ (right) for $Z \to \tau\tau$ candidates selected by the LHCb experiment.

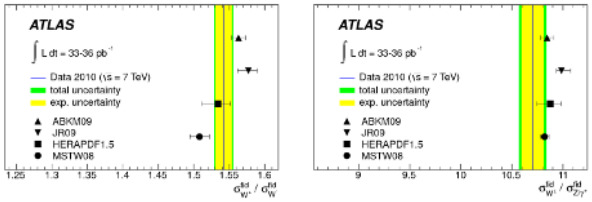

Figure 3. Cross section ratios $\sigma(W^+)/\sigma(W^-)$ (left) and $\sigma(W)/\sigma(Z)$ (right) in the fiducial phase space of the measurement. Experimental values are compared with the theoretical predictions computed at NNLO with several sets of PDF.

The angular coverage in pseudorapidity[1] of the lepton is $|\eta(\mu)| < 2.4$ (2.1) for ATLAS (CMS) and $|\eta(e)| < 2.5$ both for experiments. Some analysis are extended to the most forward region $|\eta(e)| < 5$ where the electron is identified in the endcap calorimeters, but with no tracking information. Transverse momentum thresholds in LHCb are similar, $p_T(\ell) > 20\,\text{GeV}$ although its forward configuration provides coverage for muon and electron identification in the range $2 < |\eta(\ell)| < 4.5$. The Z peak region is defined as the interval $66 < M_{\ell\ell} < 116\,\text{GeV}$ for ATLAS ($60 < M_{\ell\ell} < 120\,\text{GeV}$ for CMS and LHCb) to minimize the contribution from γ^* exchange.

Several selected results obtained recently by the LHC experiments are briefly described in the following paragraphs. Most of them come from the analysis of the data collected at $\sqrt{s} = 7\,\text{TeV}$ in 2011. Few results are from the first data taken at $\sqrt{s} = 8\,\text{TeV}$ in 2012.

2 Total cross sections and cross section ratios

CMS has measured the inclusive W and Z cross section at 8 TeV [5]. A dedicated machine configuration was deployed at the beginning of the 2012 LHC run to accumulate a dataset with low pileup and low transverse momentum trigger thresholds in experimental conditions similar to those in 2010 run. The instantaneous luminosity was reduced and hence the pileup, by separating the LHC beams in the transverse plane to diminish the effective overlap between them. A dataset corresponding to an integrated luminosity of $18.7\,\text{pb}^{-1}$ was recorded. The analysis strategy followed closely the analysis carried out at $\sqrt{s} = 7\,\text{TeV}$ [6]. The numerical results for the total W and Z cross sections times the relevant leptonic branching fractions are shown graphically in figure 1. The systematic uncertainty is $\sim 3.8\%$ in the electron channel and $\sim 2.5\%$ in the muon channel (excluding the luminosity uncertainty). Measured cross sections are in agreement with theoretical predictions computed with FEWZ at NNLO and MSTW08NNLO [7] set of PDF, the precision of the prediction is of the order of $2-3\%$.

[1]The pseudorapidity is defined as $\eta = -\ln(\tan(\theta/2))$ where θ is the polar angle of the track.

LHCb has analyzed the full data set collected in 2011 ($\sim 1\,\text{fb}^{-1}$) and measured the Z total cross section in the three leptonic decay modes ($Z \to \mu^+\mu^-$ [9], e^+e^- [10] and $\tau^+\tau^-$ [11]). Final states where the τ decays into an electron or a muon, and also hadronically, are selected. Figure 2 illustrates the invariant mass distribution of the decay products of the two τ candidates, for two different $\tau\tau$ final states. Results obtained in the three different leptonic decay modes are compatible and are in agreement with the theoretical prediction derived with FEWZ at NNLO.

Cross section ratios are measured with a higher precision as some uncertainties cancel in the ratio. Figure 3 shows the cross section ratios W^+/W^- and W/Z measured by ATLAS with the data set collected in 2010, at $\sqrt{s} = 7\,\text{TeV}$ and corresponding to an integrated luminosity of 36 pb^{-1} [8]. The total uncertainty is 0.9% for the W^+/W^- ratio and 1.3% for the W/Z ratio. Measurements in the figure are compared with four different sets of PDF and one can observe some significant differences among them, specially for the W^+/W^- ratio as it is more sensitive to the differences between the up and down quark distributions.

3 W charge asymmetry

The higher production rate of W^+ bosons with respect to W^- bosons, evidenced by a $\sigma(W^+)/\sigma(W^-)$ significantly larger than one is due to the presence of two u and one d valence quarks in the proton, modulated by the difference between the u and d quark PDF. This difference in production is further studied as a function of the pseudorapidity of the lepton from the W decay in terms of an asymmetry

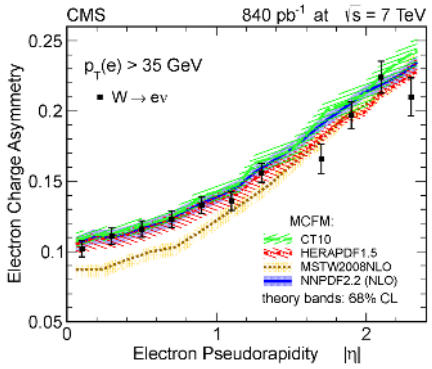

Figure 4. Measured electron charge asymmetry ($p_{\mathrm{T}} > 35\,\mathrm{GeV}$) and comparison to the predictions of different PDF models.

observable, defined as:

$$\mathcal{A}(\eta) = \frac{(\sigma(\eta)(\mathrm{W}^+) - \sigma(\eta)(\mathrm{W}^-))}{(\sigma(\eta)(\mathrm{W}^+) + \sigma(\eta)(\mathrm{W}^-))}$$

The measurement of the asymmetry provides constraints on the u, d, $\bar{\mathrm{u}}$ and $\bar{\mathrm{d}}$ in the range $10^{-3} < x < 10^{-1}$.

Most recent measurements come from CMS [12] from the analysis of a data sample corresponding to $840\,\mathrm{pb}^{-1}$ of data in the electron channel. The analysis strategy is the same followed in the inclusive analysis but with the data further separated according to the sign and pseudo-rapidity of the electron from the W candidate. Figure 4 shows the measured asymmetry, together with the theoretical predictions obtained with MCFM [13] at NLO, and various sets of parton distribution functions. There is a general agreement with the predictions. Discrepancies observed in the central region $|\eta| \lesssim 1$ with predictions using MSTW (also observed in the comparison with the ATLAS results [8]) are understood and solved, and updated versions of MSTW08 PDF [14] exhibit a good agreement with the experimental results. LHCb has recently provided [15] extrapolated values of their published asymmetries to the fiducial region of ATLAS and CMS for comparison and an excellent agreement between the different experiments in the common region is observed.

4 Z differential distribution with rapidity

The LHCb collaboration has also measured the Z differential cross section as a function of the rapidity of the dilepton system in the very forward region in the dimuon and dielectron channels [9, 10]. Figure 5 shows the differential cross section in the dimuon channel. Measured values are in agreement with NNLO calculations computed with FEWZ and various sets of PDF (Figure 5) and also with predictions computed with RESBOS [16] and POWHEG. It is in very good agreement with all three predictions. Extrapolated values to the fiducial region of ATLAS are also in agreement with the measurements from this experiment [8].

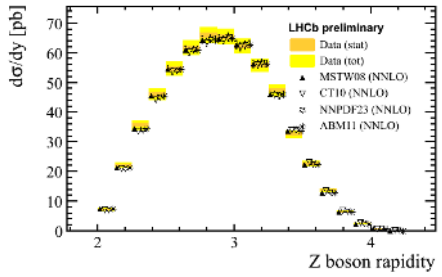

Figure 5. Differential cross-section for $\mathrm{Z} \to \mu\mu$ as a function of rapidity of the Z boson. Superimposed are the fixed order NNLO predictions from FEWZ using several PDF sets.

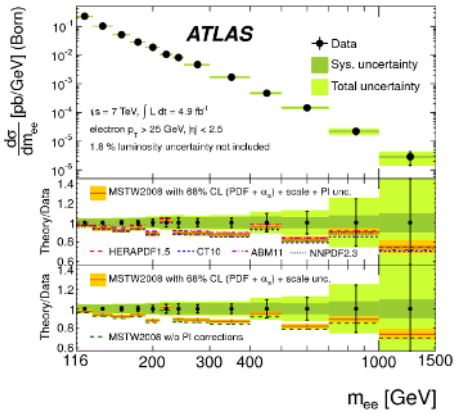

Figure 6. Drell-Yan differential cross-section measured by ATLAS.

5 Drell-Yan differential cross section

The Drell-Yan process produces dilepton pairs over a wide range of invariant mass $M_{\ell\ell}$. It constitutes an excellent test of pQCD within the Standard Model and gives access to x regions where PDF are poorly known. In addition, measuring the Drell-Yan spectrum is important as it is a copious background for many other measurements at the LHC and for searches for new physics beyond the Standard Model, such as the production of high mass dilepton resonances.

ATLAS has measured the absolute differential cross section in the dielectron channel [17]. It concentrates in the high mass region $116 < M_{\mathrm{ee}} < 1500\,\mathrm{GeV}$. The differential cross section is given in the fiducial region of the measurement after correction for lepton reconstruction, identification and trigger efficiencies. Systematic uncertainties are about 4% for $M_{\mathrm{ee}} = 116\,\mathrm{GeV}$ and are dominated by lepton reconstruction and energy measurements effects. It is of the order of $5-6\%$ for $M_{\mathrm{ee}} \sim 400\,\mathrm{GeV}$, and increases up to $\sim$ 10% for the highest M_{ee} bin. Figure 6 shows the differential cross section at Born level, i.e. after correction for QED FSR effects within the fiducial region. It is compared with theoretical predictions at NNLO from FEWZ using several sets of PDF. A general agreement is observed.

CMS has recently measured the Drell-Yan differential cross section [18] in the dimuon and dielectron chan-

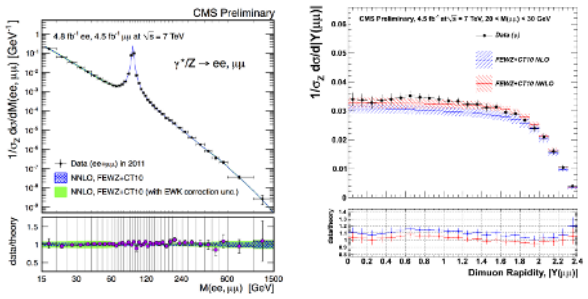

Figure 7. (Left) Combined Drell-Yan differential cross section measurement in the dimuon and dielectron channels normalized to the Z-peak region. (Right) Double differential cross section as a function of dimuon rapidity in the range $20 < M_{\mu\mu} < 30\,\text{GeV}$ and comparison with theory expectations at NLO and NNLO from FEWZ using CT10 PDF set.

nel in a very large range of dilepton invariant masses, $15\,\text{GeV} < M_{\ell\ell} < 1500\,\text{GeV}$. The measurement is normalized to the cross section in the Z peak region (60, 120) GeV to diminish the associated uncertainties. Figure 7 (left) shows the combined Drell-Yan spectrum fully unfolded for detector resolution and FSR effects and extrapolated to the full phase space. Uncertainties in the dimuon channel are dominated by the uncertainties in the efficiency corrections (1%), and in the FSR correction (0.3%). The most important source of systematic uncertainties in the dielectron channel is associated to the energy scale corrections (0.7%). There is an excellent agreement with the theoretical predictions at NNLO pQCD (FEWZ+CT10 [19]) over several orders of magnitude. A NNLO description is essential to describe the low mass region since a large fraction of the events selected in the low mass bins corresponds to high-p_{T} lepton pairs accompanied by hard jets. The analysis is extended in the dimuon channel to measure the normalized double differential cross section with respect to the mass and rapidity of the dimuon system. The rapidity bins are optimized to reduce event migrations between bins. The double differential cross section is quoted in the detection fiducial region to reduce any model dependences and to increase the constraining power of the measurement. Normalized distributions are compared with theoretical predictions from FEWZ using CT10 PDF set, at two different orders of evolution in pQCD (NLO and NNLO). From the comparison in the first mass bin (Figure 7 (right)) it is clear that the NLO theoretical prediction does not describe properly the observed spectrum whereas the NNLO calculation is able to restore the agreement with data. Normalized double differential distributions are also compared with predictions using several sets of NNLO PDF sets. These data is useful for future PDF analysis, specially for large-x regions where PDF are poorly known.

The measurement of the Drell-Yan differential cross section, $\text{d}\sigma/\text{d}M_{\mu\mu}$ by LHCb [20] in the forward rapidity region and in the low mass range ($5 < M_{\mu\mu} < 120\,\text{GeV}$) complements the previous ones as it probes down to regions of $x = 8 \times 10^{-6}$. Measurements are successfully reproduced by calculations at NLO (FEWZ and DYNNLO) and the different PDF sets studied.

6 Z p_{T} differential distribution

In hadronic collisions W and Z vector bosons are produced with a transverse momentum with respect to the beam axis balancing initial state QCD radiation of quarks and gluons. The high p_{T} region ($p_{\text{T}} > M_{\text{Z}}$), is determined by hard parton emission and a perturbative QCD description at a fixed order of α_{s} is adequate. At low p_{T}, contributions at higher orders of α_{s} describing the production of soft gluons grow in importance and resummation of the divergent logarithmic terms is needed to derive a finite cross section. Other approaches like Parton Shower aim to describe this low p_{T} region tuning certain parameters that govern the underlying event description.

The dataset collected at 8 TeV in the dedicated run with low luminosity has been analyzed by CMS to study the shape of the Z differential cross section, $1/\sigma\text{d}\sigma/\text{d}p_{\text{T}}$ [21] in the dimuon channel up to a p_{T} of the dimuon system of 600 GeV. The measured p_{T} distribution is corrected for bin migration effects due to detector resolution and from final state radiation using a matrix based unfolding procedure. The measurement is dominated by statistical uncertainties. The spectrum in the reduced fiducial phase space is compared with the predictions from several Montecarlo codes and it is found that RESBOS provides a good description of the data, better than MADGRAPH [22] or POWHEG associated to a parton shower as described by PYTHIA [23]. The low p_{T} region is scrutinized to establish the performance of several underlying event descriptions.

The study of the Z boson dynamics in terms of angular variables of the lepton tracks, which are reconstructed with very high precision, has been proposed recently [24]. Results are available for the Z differential cross section with respect to the variable $\phi^*_\eta = \tan(\phi_{\text{acop}}/2) \times \sin\theta^*_\eta$, where $\phi_{\text{acop}} = \pi - \Delta\phi$ and $\Delta\phi$ is the difference in the azimuthal angle of the two leptons from the Z decay. The angle θ^*_η defined as $\cos\theta^*_\eta = \tanh[(\eta^- - \eta^+)/2]$ where η^- and η^+ are the pseudorapidities of the two leptons, is a measurement of the scattering angle of the leptons with respect to the proton beam direction in the rest frame of the dilepton system. The ϕ^*_η variable is correlated with $p^{\text{Z}}_{\text{T}}/M_{\ell\ell}$.

ATLAS has measured [25] the normalized differential cross section $1/\sigma\text{d}\sigma/\text{d}\phi^*_\eta$ in the ϕ^*_η range $(10^{-3}, 3)$ (Figure 8, left). After correction for bin-migration effects and FSR the spectrum is compared with theoretical predictions and it is found that RESBOS reproduces the data within 2% (5%) for $\phi^*_\eta < (>)$ 0.1. Predictions [26] provided by the same authors that proposed this optimal value are also compared, and they are in agreement within the uncertainty of the prediction, still quite large. The spectrum in the region $\phi^*_\eta > 0.1$ is compared with predictions computed at fixed order of perturbation theory with FEWZ and it is found to be low by $\sim 10\%$. Differential cross sections in several lepton pseudorapidity regions are also compared with predictions using several sets of PDF and generator tunes aiming to describe the underlying event.

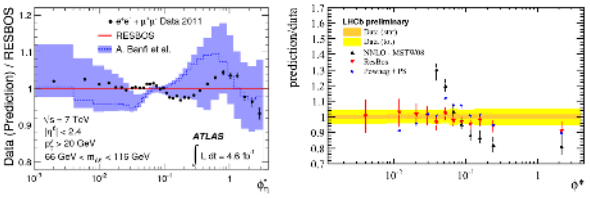

Figure 8. (Left) Ratio of the combined normalized differential cross section $1\sigma^{\rm fid}{\rm d}\sigma^{\rm fid}/{\rm d}\phi^*$ measured in ATLAS to predictions from RESBOS and from [26] as a function of ϕ^*. (Right) Ratio of the QCD predictions (RESBOS, FEWZ and POWHEG+PS) to data for the differential cross section ${\rm d}\sigma/{\rm d}\phi^*$ measured by LHCb.

Similar conclusions are reached in the LHCb analysis [9] where the differential cross section ${\rm d}\sigma/{\rm d}\phi^*_\eta$ is presented (Figure 8, right). The theoretical calculation at NNLO from FEWZ overshoots the observation for $\phi^*_\eta < 0.1$ and undershoots it for $\phi^*_\eta > 0.1$. RESBOS correctly predicts the spectrum over the whole range. Other predictions, as POWHEG+Parton Shower lays within 10% of the observed values.

7 Electroweak observables

The angular distribution of the leptons from the Drell-Yan process is determined by the vector and axial-vector couplings of the quarks and leptons to the Z boson and on the electric charge of the fermions. An asymmetry parameter can be defined as $A_{\rm FB} = (\sigma_{\rm F}-\sigma_{\rm B})/(\sigma_{\rm F}+\sigma_{\rm B})$ where $\sigma_{\rm F}$ and $\sigma_{\rm B}$ are the total cross sections for forward and backward events, depending on the angle of emission of the lepton relative to the quark momentum in the dilepton center of mass system. $A_{\rm FB}$ is small near the Z peak.

The forward-backward asymmetry in the dimuon and dielectron channels has been measured recently by CMS [27], in the mass range: $40 < M_{\ell\ell} < 400\,{\rm GeV}$. The analysis is done in several rapidity bins of the dilepton system as the sensitivity to the asymmetry is larger for dileptons produced at large rapidities. Raw asymmetries are corrected for FSR, mass resolution, efficiencies and other detector effects, and unfolded to Born level, where the unfolding is done independently for each rapidity bin. The effect of the unfolding is maximal just below and above the Z peak. A good agreement with the standard model is observed (Figure 9).

ATLAS has published recently [28] the asymmetry measured in the dimuon and dielectron channels. Electrons detected in the forward region ($2.5 < |\eta({\rm e})| < 4.9$) are also included in the analysis giving access to a region where the dilution due to the impossibility to define precisely the direction of the incoming quark is minimized. The asymmetry is already visible at raw level in the data sample with one forward electron (Figure 10). The asymmetry is measured in a wide range of dilepton invariant mass $66 < M_{\ell\ell} < 1000\,{\rm GeV}$ (<250 GeV for the category with a very forward electron) and unfolded to Born level correcting for FSR, detector and dilution effects. All of the resulting $A_{\rm FB}$ spectra are consistent with the corresponding Standard Model predictions. Several Standard Model parameters can be extracted from the measured $A_{\rm FB}$ distribution. One of them is the effective weak mixing angle, $\sin^2\theta^{\rm eff}_{\rm W}$. ATLAS has extracted the value of $\sin^2\theta^{\rm eff}_{\rm W}$ from the measured $A_{\rm FB}$ spectra by comparing the raw asymmetry in the mass range (70, 250) GeV to Montecarlo predictions produced with varying initial values of the weak mixing angle. The final combined value $\sin^2\theta^{\rm eff}_{\rm W} = 0.2297\pm0.0004\pm0.0009$, has already a precision comparable with the ultimate measurements of Tevatron experiments and is found to be in agreement with previous determinations.

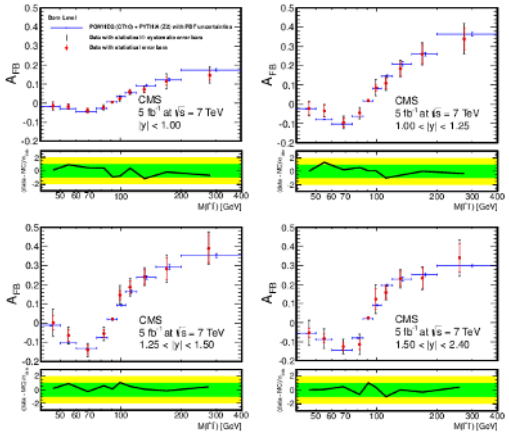

Figure 9. Combined ($\mu^+\mu^-$ and $\rm e^+e^-$) measurement of $A_{\rm FB}$ at the Born level in four $|y_{\rm Z}|$ bins from CMS.

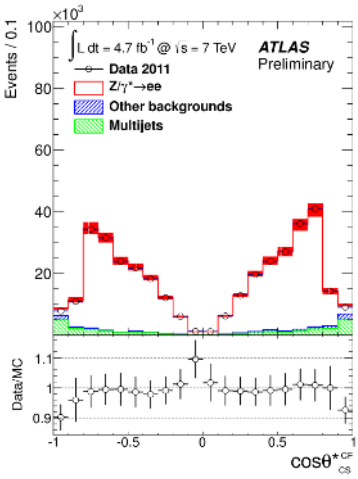

Figure 10. Distribution of the scattering angle of the electron in the dielectron channel where one of the electrons is detected in the very forward region of the ATLAS experiment.

Acknowledgements

The author wish to thank the ATLAS (Standard Model), CMS (Standard Model Physics) and LHCb (QCD, Electroweak and Exotica) working groups and convenors for their help preparing this talk.

References

[1] K. Melnikov and F. Petriello, *Electroweak gauge boson production at hadron colliders through $O(\alpha_s{}^2)$*, Phys. Rev. D74 (2006) 114017, arXiv: hep-ph/0609070.

[2] S. Catani, L. Cieri, G. Ferrera, D. de Florian and M. Grazzini, *Vector boson production at hadron colliders: a fully exclusive QCD calculation at NNLO*, Phys. Rev. Lett. 103 (2009) 082001, arXiv:0903.2120.

[3] S. Alioli, P. Nason, C. Oleari and E. Re, *NLO vector-boson production matched with shower in POWHEG*, J. High Energy Phys. 07 (2008) 060, arXiv: 0805.4802.

[4] S. Frixione and B.R. Webber, *Matching NLO QCD computations and parton shower simulations*, J. High Energy Phys. 06 (2002) 029, arXiv:0805.4802.

[5] CMS Collaboration, *W and Z inclusive cross sections at 8 TeV*, CMS-PAS-SMP-12-011, https://cdsweb.cern.ch/record/1460098.

[6] CMS Collaboration, *Measurements of Inclusive W and Z Cross Sections in pp Collisions at $\sqrt{s}$ = 7 TeV with the CMS experiment*, J. High Energy Phys. 10 (2011) 132, arXiv:1107.4789.

[7] A.D. Martin, W.J. Stirling, R.S. Thorne and G. Watt, *Parton distributions for the LHC*, Eur. Phys. J. C63 (2009) 189, arXiv: 0901.0002.

[8] ATLAS Collaboration, *A measurement of the total W and Z/γ^* cross sections in the e and μ decay channels in pp collisions at $\sqrt{s}$ = 7 TeV with the ATLAS detector*, Phys. Rev. D85 (2012) 072004, arXiv:1109.5141.

[9] LHCb Collaboration,*Measurement of the cross-section for* $Z \rightarrow \mu^+\mu^-$ *production with 1 fb^{-1} of pp collisions at $\sqrt{s}$ = 7 TeV*. LHCb-CONF-2013-007, http://cds.cern.ch/record/1537825.

[10] LHCb Collaboration, *Measurement of the cross-section for* $Z \rightarrow e^+e^-$ *production in pp collisions at $\sqrt{s}$ = 7 TeV*. J. High Energy Phys. 02 (2013) 106.

[11] LHCb Collaboration, *A study of the Z production cross-section in pp collisions at $\sqrt{s}$ = 7 TeV using tau final states*, J. High Energy Phys. 01 (2013) 111.

[12] CMS Collaboration, *W differential lepton charge asymmetry at 7 TeV*, Phys. Rev. Lett. 109 (2012) 111806, arXiv:1206.2598.

[13] J. M. Campbell and R. Ellis, *MCFM for the Tevatron and the LHC*, Nucl. Phys. Proc. Suppl. 205 (2010) 10, arXiv: 1007.3492.

[14] A.D.Martin et al., *Extended Parameterisations for MSTW PDFs and their effect on Lepton Charge Asymmetry from W Decays*, Eur. Phys. J. C (2013) 73:2318, arXiv:1211.1215.

[15] LHCb Collaboration, *Graphical comparison of the LHCb measurements of W and Z boson production with ATLAS and CMS*, LHCb-CONF-2013-005, http://cdsweb.cern.ch/record/1529709.

[16] C. Balazs and C.-P. Yuan, *Soft gluon effects on lepton pairs at hadron colliders*, Phys. Rev. Lett. 79 (1997), arXiv: hep-ph/9703405.

[17] ATLAS Collaboration, *Measurement of the high-mass Drell-Yan differential cross-section in pp collisions at $\sqrt{s}$ = 7 TeV with the ATLAS detector*, CERN-PH-EP-2013-064, arXiv:1305.4192.

[18] CMS Collaboration, *Drell-Yan differential cross sections at 7 TeV*, CMS-PAS-SMP-13-003, https://cdsweb.cern.ch/record/1543468.

[19] H.-L. Lai, M. Guzzi, J. Huston, Z. Li, P. Nadolsky, J. Pumplin and C.-P. Yuan, *New parton distributions for collider physics*, Phys. Rev. D82 (2010) 074024, arXiv:1007.2241.

[20] LHCb Collaboration, *Inclusive low mass Drell-Yan production in the forward region at $\sqrt{s}$ = 7 TeV*, CERN-LHCb-CONF-2012-016, http://cdsweb.cern.ch/record/1434424.

[21] CMS Collaboration, *Z transverse momentum distribution at 8 TeV*, CMS-PAS-SMP-12-025, https://cdsweb.cern.ch/record/1528579.

[22] J. Alwall, M. Herquet, F. Maltoni, O. Mattelaer and T. Stelzer, *MadGraph5: Going Beyond*, J. High Energy Phys. 06 (2011) 128, arXiv: 1106.0522.

[23] T. Sjöstrand, S. Mrenna, S. and P.Z. Skands, *PYTHIA 6.4 Physics and Manual*, J. High Energy Phys. 05 (2006) 26, arXiv: hep-ph/0603175.

[24] A. Banfi et al., *Optimisation of variables for studying dilepton transverse momentum distributions at hadron colliders*, Eur. Phys. J. C 71 (2011) 1600, arXiv: 1009.1580.

[25] ATLAS Collaboration, *Measurement of angular correlations in Drell-Yan lepton pairs to probe Z/γ^* boson transverse momentum at $\sqrt{s}$ = 7 TeV with the ATLAS detector*, Phys. Lett. B 720 (2013) 32-51, arXiv:1211.6899.

[26] A.Banfi et al., *Predictions for Drell-Yan ϕ^* and Q_T observables at the LHC*, Phys. Lett. B 715 (2012) 152, arXiv:1205.4760.

[27] CMS Collaboration, *Drell-Yan differential forward-backward asymmetry at 7 TeV*, Phys. Lett. B 718 (2013) 752, arXiv:1207.3973.

[28] ATLAS Collaboration, *A_{FB} of Z/γ into muon and electron pairs and extraction of* $\sin^2\theta_W$, ATLAS-CONF-2013-043, http://cdsweb.cern.ch/record/1544035.